mechanistically. It returns to the original point of this paper and to the design of *trans*-$[Ru^{VI}(tpy)(O)_2(H_2O)]^{2+}$ as a potential cis-directed four-electron oxidant. In order for this reactivity to appear, the transfer of the remaining oxo group at Ru(IV) must occur to the plane of the tpy ligand following reduction of Ru(VI) to Ru(IV). This could occur, for example, by intramolecular proton transfer. These issues are currently under investigation.

Acknowledgments are made to the National Science Foundation under Grant CHE-8906794 for support of this research. We also acknowledge Dr. R. A. Binstead for helpful discussions and Dr. J. R. Schoonover for assistance with the Raman experiments.

Contribution from the Departments of Chemistry, University of Leicester, Leicester LE1 7RH, U.K., and University of New Hampshire, Durham, New Hampshire 03824-3598

The Iron(II)–Diimine Complex $[Fe(CH_3N{=}CHCH{=}NCH_3)_3]^{2+}$: Its Structure and Its Solvation and Reactivity in Aqueous–Organic Solvent Mixtures

Michael J. Blandamer,[†] John Burgess,[†] John Fawcett,[†] Pilar Guardado,[†,‡] Colin D. Hubbard,[*,§] Sumchairuk Nuttall,[†] Lesley J. S. Prouse,[†] Stojan Radulović,[†] and David R. Russell[†]

Received March 21, 1991

Tris (*N,N'*-dimethylglyoxal diimine)iron(II) ($Fe(gmi)_3^{2+}$) salts have been prepared, and the structure of the tetrafluoroborate salt has been determined by an X-ray diffraction study. $Fe(gmi)_3(BF_4)_2$, $C_{12}H_{24}N_6B_2F_8Fe$, is rhombohedral and crystallizes in space group $R\bar{3}c$, and there are six molecules per cell. In addition the structure of $[Fe(bmi)_3](ClO_4)_2$ ($C_{18}H_{36}N_6O_8Cl_2Fe$, trigonal, space group $P\bar{3}c1$, two molecules per cell), where the bmi ligand (*N,N'*-dimethyl-2,3-butanedione diimine) is the dimethyl analogue of gmi, has been determined so that together with available structural data for other iron(II)–diimine complexes the general reactivity of the $Fe(gmi)_3^{2+}$ cation on the basis of structural information may be ascertained. Dissociation of $Fe(gmi)_3^{2+}$ in the presence of hydroxide ion has been studied spectrophotometrically. The second-order rate constant, k_2 (the reaction is first order in both reactants under the conditions studied), was determined for several aqueous mono-ol mixtures and in aqueous acetone. The trend of a sharp increase in k_2 with increasing organic cosolvent content was observed; destabilization of hydroxide is a significant contributing factor. Solubility measurements were made using the perchlorate salt of the complex ion. These results, in conjunction with the TATB extrathermodynamic assumption, afforded the transfer chemical potentials for the initial state, and in combination with appropriate kinetic data those for the transition state. The reactivity trends are controlled more or less equivalently by an increasing destabilization of the overall initial state and a stabilized transition state with increasing cosolvent for aqueous ethanol, 2-propanol, and *tert*-butyl alcohol mixtures. Kinetic measurements at pressures up to 1 kbar yielded ΔV^* of +16 $cm^3\ mol^{-1}$ for dissociation by hydroxide ion in aqueous solution. ΔV^* is lowered by all cosolvents added, the value declining to +4 $cm^3\ mol^{-1}$ at the highest practicable cosolvent concentration.

Introduction

Medium effects on reactivity have been studied for a large number of reactions, organic and inorganic. Explanations of these effects have been offered in terms of a great variety of solvent properties and parameters. Most treatments deal with rate constant and activation parameter trends, but several authors have recognized that such kinetic parameters are composite quantities, representing differences between effects on initial and transition states.[1,2] Analysis of solvent effects on reactivities in these terms should lead to fuller understanding. In parallel with this approach, it is becoming increasingly recognized that solvation may have a marked effect on the pressure dependence of reactivities.[3] For a reaction of established mechanism, solvation effects can be probed through variation of activation volume with solvent nature or composition. These two approaches are complementary, in that the initial-state–transition-state analysis gives information on solvation changes for the initial state and transition state separately, on transfer from one medium to another, whereas the activation volume can give an idea of solvation changes on going from the initial state to the transition state in a given medium. This is illustrated in Figure 1, which also recalls that thermodynamic measurements, such as solubilities, are required to obtain information on transfer of the initial state, and solvent effects on the transition state can be derived from these measurements and the observed rate constants.[2] In the present paper we illustrate these approaches through the study of solvent effects on base hydrolysis of a low-spin iron(II)–diimine complex in several series of binary aqueous solvent mixtures.

The kinetics of substitution at the low-spin iron(II)–diimine complexes $Fe(phen)_3^{2+}$ (phen = **1**) and $Fe(bpy)_3^{2+}$ (bpy = **2**) have been extensively studied since the early days of inorganic kinetics.[4] The first studies were in aqueous solution, but subsequently solvolysis, base hydrolysis, and nucleophilic attack by cyanide have been studied in many nonaqueous and mixed aqueous media.[5] The range of diimine ligands can readily be extended by the use of Schiff bases (sb) derived from pyridine-2-aldehyde and 2-keto derivatives, **3** with R = H, CH_3, C_6H_5 and R' = alkyl or aryl.[6] However, cations $Fe(sb)_3^{2+}$ of this type of ligand introduce the possible complication of *mer* and *fac* isomers; isomer mixtures or isomerization may well interfere with substitution kinetic studies (cf. racemization in parallel with substitution at optically active complexes of the $Fe(phen)_3^{2+}$ type[7]). The problem of isomeric forms may be avoided by the use of symmetrical diimines, **4**,[8] derived from α-diketones such as glyoxal (R = H) and biacetyl (butane-2,3-dione; R = CH_3), which have long been known to form very stable, intensely colored, iron(II) complexes.[9-11] Indeed,

* Author to whom correspondence should be addressed.
† University of Leicester.
‡ On leave from the Departamento de Quimica Fisica, Universidad de Sevilla, Sevilla, Spain.
§ University of New Hampshire.

(1) Parker, A. J. *Chem. Rev.* **1969**, *69*, 1.
(2) Blandamer, M. J.; Burgess, J. *Pure Appl. Chem.* **1979**, *51*, 2087; *Coord. Chem. Rev.* **1980**, *31*, 93; *Pure Appl. Chem.* **1982**, *54*, 2285; **1983**, *55*, 55.
(3) van Eldik, R. In *Inorganic High Pressure Chemistry-Kinetics and Mechanisms*; van Eldik, R., Ed.; Elsevier: Amsterdam, 1986; Section 1.5. Isaacs, N. S. *Liquid Phase High Pressure Chemistry*; Wiley: New York, 1981; Chapter 4.
(4) Lee, T. S.; Kolthoff, I. M.; Leussing, D. L. *J. Am. Chem. Soc.* **1948**, *70*, 2348, 3596. Krumholz, P. *Nature (London)* **1949**, 163, 724. Baxendale, J. H.; George, P. *Ibid.* **1949**, *163*, 725; *Trans. Faraday Soc.* **1950**, *46*, 736. Basolo, F.; Hayes, J. C.; Neumann, H. M. *J. Am. Chem. Soc.* **1954**, *76*, 3807. Krumholz, P. *J. Phys. Chem.* **1956**, *60*, 87. Dickens, J. F.; Basolo, F.; Neumann, H. M. *J. Am. Chem. Soc.* **1957**, *79*, 1286.
(5) Burgess, J.; Pelizzetti, E. *Gazz. Chim. Ital.* **1988**, *118*, 803.
(6) Bähr, G.; Thämlitz, H. *Z. Anorg. Allg. Chem.* **1955**, *282*, 3. Bähr, G.; Döge, H.-G. *Ibid.* **1957**, *292*, 119.
(7) Yamagishi, A. *Inorg. Chem.* **1986**, *25*, 55.
(8) Pechmann, H. V. *Chem. Ber.* **1888**, *21*, 1412.

0020-1669/92/1331-1383$03.00/0

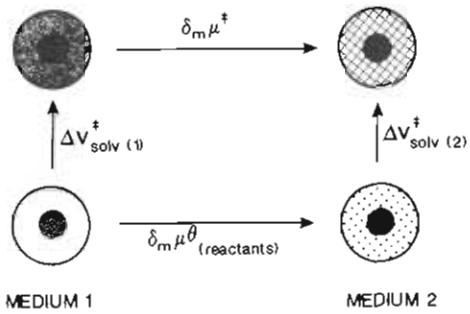

Figure 1. Interrelation between solvent effects on initial and transition states and derivation of relevant information from medium and pressure effects on reactivities and medium effects on solvation of reactants. ΔV^{*}_{solv} is the solvation contribution to the observed activation volume ΔV^{*}_{obs}. $\delta_m\mu^{\theta}$ is the change in chemical potential per mole (due to solvation changes), upon transferring reactants from medium 1 to medium 2.

the first intensely colored iron(II)–diimine complex described by Blau in 1898[12] was almost certainly the tris complex of ligand **5**, a cyclic derivative of **4**. The first fully characterized examples had R′ = CH_3, but a range of complexes can be built up by varying the nature of R′ (including R′ = aryl[8,13]) and, indeed, of R (e.g. by the use of benzil R = C_6H_5) or of cyclohexane-1,2-dione (R plus R = $-(CH_2)_4-$)[14]). In practice the iron(II) complexes of aryl derivatives of **4** are too labile for kinetic convenience, while $Fe(bmi)_3^{2+}$ (bmi = **4**, R = R′ = CH_3) undergoes aquation in dilute acid and base hydrolysis extremely slowly. This narrows the choice of substrate down greatly, with $Fe(gmi)_3^{2+}$ (gmi = **4**, R = H, R′ = CH_3) as our complex of choice. Kinetics of racemization and, to a limited extent, aquation of this complex have been established, in water and some nonaqueous solvents.[15]

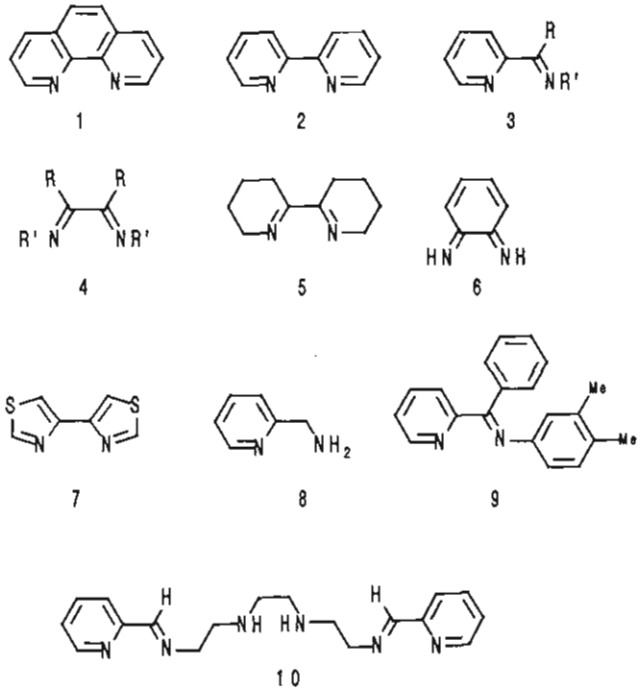

In this paper we report rate constants for base hydrolysis of $Fe(gmi)_3^{2+}$ in binary aqueous solvent mixtures, for cosolvents methanol, ethanol, 2-propanol, and *tert*-butyl alcohol, at atmospheric pressure and at pressure up to (in most cases) 1.03 kbar. In order to analyze the reactivity trends at 1 atm, we have measured solubilities of $[Fe(gmi)_3](ClO_4)_2$ and, thence, derived transfer chemical potentials. Both these transfer chemical potentials and the high-pressure kinetics results show trends with solvent composition which indicate a key role for solvent structural effects and their consequences on reactant and transition-state solvation.

There are reasons for being slightly skeptical of accepting the simple tris(diimine-*N,N*) structure that seems intuitively obvious for the $Fe(gmi)_3^{2+}$ cation. There is an unexpectedly complicated sequence of color changes in its preparation,[9] there is the possibility of the addition of water across one of the ligand C=N bonds, there is the remote possibility of the C,N-bonding reported in the iridium(III)–2,2′-bipyridyl system,[16,17] and indeed there are other rather odd bonding modes now well established for diimines coordinated to low oxidation state metals.[18] It therefore seemed wise to carry out a single-crystal X-ray diffraction structure determination on a salt of the $Fe(gmi)_3^{2+}$ cation. The results of such a determination, on the tetrafluoroborate salt (attempts to solve the structure of the hexafluorophosphate salt had been unsuccessful), are reported here. We also report the results of an X-ray diffraction structure determination on a single crystal of the closely related $Fe(bmi)_3^{2+}$ cation (less convenient than $Fe(gmi)_3^{2+}$ for study of kinetics of base hydrolysis, not only because it reacts much more slowly but also because it is more prone to oxidation[18]) in the form of its perchlorate salt. The structures of these two cations are compared with each other with particular reference to relations between bond lengths and implied bond orders on the one hand and the known large difference in reactivities on the other. The geometries of these two tris(diimine) cations are also compared with those for other low spin iron(II)–diimine complexes.

Experimental Section

Materials. The salts $[Fe(gmi)_3](ClO_4)_2$ and $[Fe(bmi)_3](ClO_4)_2$ were prepared from ammonium iron(II) sulfate, aqueous glyoxal, and aqueous methylamine solution, or butane-2,3-dione dissolved in aqueous ethanol, with subsequent precipitation, as described earlier.[19] The perchlorate salts are potentially hazardous and should be prepared in small quantities and be treated cautiously. They were checked by comparison of their visible region spectra with published details.[20] The perchlorate salts were used for kinetic and solubility measurements. In the case of the complex of gmi it proved impossible to obtain a crystal of the perchlorate of sufficient quality for X-ray diffraction studies. The crystal structure was determined on a crystal of the tetrafluoroborate salt, obtained by slow evaporation and crystallization of a solution of $[Fe(gmi)_3](BF_4)_2$. The alcohols and acetone used to make up the solvent mixtures were of the best commercially available grade, dried by standard procedures.[21] Mixed solvent media were made up by volume before mixing: 90% v/v means, for example, 90 mL of cosolvent mixed with 10 mL of water. The inorganic reagents used in preparing solutions for the kinetic studies were AnalaR materials.

Kinetics. Rate constants were determined using the apparatus and procedures described earlier, both for atmospheric[22] and for high-pressure runs.[23,24] The wavelength used for monitoring kinetics was 554 nm.

Solubilities. Saturated solutions were prepared by gently agitating sealed tubes containing the appropriate solvent medium with a generous

(9) Krumholz, P. *J. Am. Chem. Soc.* **1953**, *75*, 2163; *Struct. Bonding (Berlin)* **1971**, *9*, 139.
(10) Busch, D. H.; Bailar, J. C. *J. Am. Chem. Soc.* **1956**, *78*, 1137.
(11) Chum, H. L.; Rabockai, T. *Inorg. Chim. Acta* **1976**, *19*, 145.
(12) Blau, P. *Monatsh. Chem.* **1898**, *19*, 647.
(13) Bähr, G. Z. *Anorg. Allg. Chem.* **1951**, *267*, 137. Bähr, G.; Kretzer, A. *Ibid.* **1951**, *267*, 161.
(14) Krumholz, P.; Serra, O. A.; de Paoli, M. A. *Inorg. Chim. Acta* **1975**, *15*, 25. Baggio-Saitovich, E.; de Paoli, M. A. *Ibid.* **1976**, *16*, 59.
(15) Tachiyashiki, S.; Yamatera, H. *Bull. Chem. Soc. Jpn.* **1981**, *54*, 3340.
(16) Wickramasinghe, W. A.; Bird, P. H.; Serpone, N. *J. Chem. Soc., Dalton Trans.* **1981**, 1284. Constable, E. C. *Polyhedron* **1983**, *2*, 551; **1984**, *3*, 1037 and references therein.
(17) Vrieze, K.; van Koten, G. *Inorg. Chim. Acta* **1985**, *100*, 79.
(18) da Costa Ferreira, A. M. G.; Krumholz, P.; Riveros, J. M. *J. Chem. Soc., Dalton Trans.* **1977**, 896.
(19) Radulović, S. Ph.D. Thesis, University of Leicester, 1988.
(20) Schlosser, K.; Hoyer, E. *Z. Chem.* **1970**, *10*, 439; *J. Inorg. Nucl. Chem.* **1971**, *33*, 4370. Schlosser, K.; Hoyer, E.; Arnold, D. *Spectrochim. Acta* **1974**, *30A*, 1431.
(21) Gordon, A. J.; Ford, R. A. *The Chemist's Companion*; Wiley: New York, 1972.
(22) Blandamer, M. J.; Burgess, J.; Clark, B.; Duce, P. P.; Hakin, A. W.; Gosal, N.; Radulović, S.; Guardado, P.; Sanchez, F.; Hubbard, C. D.; Abu-Gharib, E. A. *J. Chem. Soc., Faraday Trans. 1* **1986**, *82*, 1471.
(23) Burgess, J.; Hubbard, C. D. *J. Am. Chem. Soc.* **1984**, *106*, 1717; *J. Chem. Soc., Chem. Commun.* **1983**, 1482.
(24) Hallinan, N.; McArdle, P.; Burgess, J.; Guardado, P. *J. Organomet. Chem.* **1987**, *333*, 77.

Table I. Experimental Details of the X-ray Diffraction Studies[a]

	$[Fe(gmi)_3](BF_4)_2$	$[Fe(bmi)_3](ClO_4)_2$
formula	$C_{12}H_{24}N_6B_2F_8Fe$	$C_{18}H_{36}N_6O_8Cl_2Fe$
fw	481.8	591.4
ρ_{calcd}, g cm^{-3}	1.552	1.480
T, °C	20	20
λ, Å	0.71073	0.71073
μ, cm^{-1}	7.52	7.60
space group	$R\bar{3}c$	$P\bar{3}c1$
Z	6	2
a, b, Å	9.852 (2)	10.017 (2)
c, Å	36.802 (7)	15.272 (4)
γ, deg	120	120
U, Å^3	3093.7	1327.1
radiation	Mo Kα (7.52 cm^{-1})	Mo Kα (7.60 cm^{-1})
scan technique	ω scan	ω scan
2θ(max), deg	54	54
no. of data collcd	2484	3042
no. of unique data used ($I \geq 3\sigma(I)$)	596	1123
R[b]	0.0421	0.0525
R_w[c]	0.0460	0.0630
R_{int}	0.0325	0.0288

[a] SHELX-76: Sheldrick, G. M. SHELX Program for Crystal Structure Determination. University of Cambridge, 1976. SHELXS86: Sheldrick, G. M. Personal communication. [b] $R = \sum||F_o| - |F_c||/\sum|F_o|$. [c] $R_w = [\sum w(|F_o| - |F_c|)^2/w|F_o|^2]^{1/2}$.

excess of $[Fe(gmi)_3](ClO_4)_2$ in a thermostat bath for several hours. Concentrations of saturated solutions were determined by carefully withdrawing aliquots after undissolved material had settled or been centrifuged to the bottom of the vessel, diluting them appropriately, and measuring absorbances in a Pye-Unicam SP 8-100 spectrophotometer.

X-ray Structure Determinations. Crystals of $[Fe(gmi)_3](BF_4)_2$ and of $[Fe(bmi)_3](ClO_4)_2$ were mounted with epoxy resin on a glass fiber (in air). In each case the crystals were deep red purple in color. The wavelength of X-rays used was 0.71073 Å, and the data were collected at 20 °C. Unit cell dimensions were determined from oscillation photographs and optimized counter angles for zero and upper layer reflections. Absorption coefficients, μ, of 7.52 and 7.60 cm^{-1} were determined for the complexes of gmi and bmi. Weissenberg diffraction geometry was employed. Intensities were measured on a Stadi-2 diffractometer. Data were corrected for Lorentz and polarization effects. Cell dimensions and other parameters are listed in Table I. An estimate of agreement between equivalent reflections is expressed through R_{int}, which is 0.0325 for the gmi complex and 0.0288 for the dimethyl analogue bmi complex. For $[Fe(gmi)_3](BF_4)_2$ data originally collected on the basis of a triclinic lattice were transformed to a rhombohedral lattice indexed on hexagonal axes; for $[Fe(bmi)_3](ClO_4)_2$ transformation from an orthorhombic cell to hexagonal cell of the trigonal space group $P\bar{3}c1$ was indicated during refinement of the structure. The structures were solved by conventional Patterson and Fourier difference techniques using the computer programs SHELX-76 and SHELXS86 and employing the conventional scattering factors. The ClO_4^- ion in $[Fe(bmi)_3](ClO_4)_2$ is disordered. Tables of atomic positional and thermal parameters and of all bond lengths, selected nonbonded contacts, and angles are available as supplementary material. The most important bond lengths and angles are tabulated in the Discussion.

Results

The decolorization of the solution of $Fe(gmi)_3^{2+}$ by hydroxide ion indicates that complete dissociation occurs, viz.

$$Fe(gmi)_3^{2+} + OH^- \rightarrow Fe(OH)^+ + 3gmi$$

In the presence of oxygen and excess hydroxide ion, the ultimate product in addition to gmi is $Fe(OH)_3$.

Kinetics. The general form of the rate law for base hydrolysis of iron(II)–diimine complexes is[25]

$$-\frac{d}{dt}[complex] = \{k_1 + k_2[OH^-] + k_3[OH^-]^2 + k_4[OH^-]^3\}[complex]$$

The k_1 term corresponds to a rate-limiting iron–nitrogen bond-breaking path and can be significant at low hydroxide concentrations especially for the less stable complexes of this type. We have established earlier that the k_1,[26] k_3,[27] and k_4 terms are negligible for base hydrolysis of $[Fe(gmi)_3]^{2+}$ in water and in aqueous methanol.[22] We have now confirmed that the k_2 term representing bimolecular attack at the complex is the only significant term under the conditions of the present investigation. Figure 2 shows plots of k_{obs} ($[Fe(gmi)_3^{2+}] \ll [OH^-]$) against hydroxide concentration for 20–60% acetone and 2-propanol cosolvents. This figure also gives an impression of the marked increase in rate constants as the proportion of the organic cosolvent is increased. Table II lists values for k_2 derived from such dependences of k_{obs} on hydroxide concentration, generally from duplicate determinations of k_{obs} at each of the five hydroxide concentrations indicated on the x axis of Figure 2. Table III includes the results of high-pressure kinetic runs reported on ratios of rate constants at high pressure to the rate constant at atmospheric pressure (k_p/k_o) for a portion of the same reaction mixture (cf. Experimental Section). Plots of logarithms of k_p/k_o against pressure are linear within experimental uncertainty; Table III also contains activation volumes (ΔV^*) derived from the pressure dependences of k_p/k_o. The uncertainties in ΔV^* are in the region of ±1 cm^3 mol^{-1}. The values of ΔV^* refer to the magnitude at 1 bar.

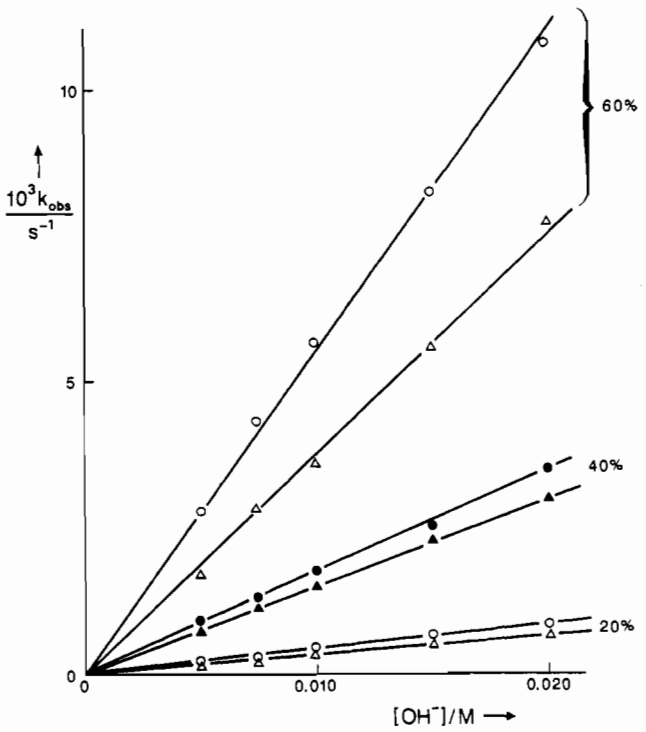

Figure 2. Dependence of observed first-order rate constants on hydroxide concentration for dissociation of $Fe(gmi)_3^{2+}$ in aqueous acetone (circles) and aqueous 2-propanol (triangles) at given volume percentages of organic cosolvent.

Solubilities. These are reported in Table IV, which also includes the derivation of transfer chemical potentials for the $[Fe(gmi)_3]^{2+}$ cation, on the TATB assumption[22] (i.e. $\delta_m\mu^\theta(Ph_4As^+) = \delta_m\mu^\theta(BPh_4^-)$).

Discussion

Structure of the $Fe(gmi)_3^{2+}$ Cation. The X-ray crystal structure determination shows that this cation does simply consist of three gmi ligands ($CH_3N{=}CHCH{=}NCH_3$) bonded to the Fe^{2+} ion. It is not possible to bond three diimine ligands of this type to a first-row transition-metal 2+ or 3+ ion to give a perfectly octahedral arrangement of the six nitrogen donor set. The bite angles, here as for $Fe(phen)_3^{2+}$, $Fe(bpy)_3^{2+}$, and several related $M(LL)_3^{n+}$

(25) Margerum, D. W.; Morgenthaler, L. P. *J. Am. Chem. Soc.* **1962**, *84*, 706.

(26) $k_1 \cong 10^{-6}$ s^{-1} at 25 °C in ref 22 and is therefore indeed negligible.

(27) E.g.: Blandamer, M. J.; Burgess, J.; Haines, R. I.; Mekhail, F. M.; Askalani, P. *J. Chem. Soc., Dalton Trans.* **1978**, 1010.

Table II. Second-Order Rate Constants ($dm^3\ mol^{-1}\ s^{-1}$) for Reaction of the $Fe(gmi)_3^{2+}$ Cation with Hydroxide in Water and in Binary Aqueous Solvent Mixtures at 298.2 K (μ = 0.33 mol dm^{-3})

	% organic cosolvent, v/v								
cosolvent	0	10	17	20	30	40	50	60	80
CH_3OH[a]	0.0052			0.0142		0.067	0.113	0.23	1.01
C_2H_5OH				0.026	0.064	0.112	0.155		
i-C_3H_7OH				0.029	0.057	0.150		0.37	
t-C_4H_9OH		0.0105	0.018	0.026	0.046	0.063	0.096		
$(CH_3)_2CO$				0.041		0.18		0.55	

[a] These values derived from k_{obs} data given in ref 22.

Table III. Ratios (k_p/k_o)[a] of Rate Constants at Pressure *P* to Those at Atmospheric Pressure for Reaction of the $Fe(gmi)_3^{2+}$ Cation with Hydroxide in Water and Binary Aqueous Solvent Mixtures and Derived Activation Volumes (ΔV^*) at 298.2 K

		$[OH^-]$,[b]	*P*, kbar					ΔV^*,
cosolvent	% v/v	mol dm^{-3}	0.34	0.68	1.03	1.21	1.38	$cm^3\ mol^{-1}$
none		0.040	0.77	0.63	0.48			+16.7
CH_3OH	20.0	0.020	0.78	0.65	0.48			+16.2
	40.0	0.010	0.81	0.65	0.51	0.43	0.39	+15.5
	50.0	0.005	0.84	0.71	0.59			+12.6
	60.0	0.002	0.91	0.80	0.70			+8.1
	80.0	0.002	0.95	0.85	0.79			+4.9
C_2H_5OH	20.0	0.010	0.86	0.74	0.57			+15.0
	30.0	0.0050	0.83	0.69	0.53			+15.0
	40.0	0.0025		0.82	0.64			
		0.0050	0.87					+10.0
	50.0	0.0015		0.92	0.81			
								+3.3
		0.0025	0.98					
i-C_3H_7OH	20.0	0.010	0.82	0.66	0.51			+15.3
	30.0	0.005	0.69					+13.7
		0.010	0.86		0.54			
	40.0	0.005	0.90	0.77	0.66			+9.7
	50.0	0.003	0.82	0.72				+7.6
	60.0	0.002		0.77				
								+5.8
		0.003	0.86					
t-C_4H_9OH	10.0	0.020	0.81	0.66	0.57			+14.9
	17.0	0.010			0.60			
								+12.2
		0.020	0.87	0.71				
	30.0	0.010	0.92	0.82	0.71			+7.4
	50.0	0.005	0.89	0.75				+4.0
$(CH_3)_2CO$	20.0	0.010	0.86	0.73	0.63			+11.0

[a] k_p/k_o is the ratio (at pressures compared with atmospheric pressure) of observed first-order rate constants at the specified hydroxide ion concentration (in all cases μ = 0.33 mol dm^{-3}). [b] The $[OH^-]$ value is that prior to pressure application.

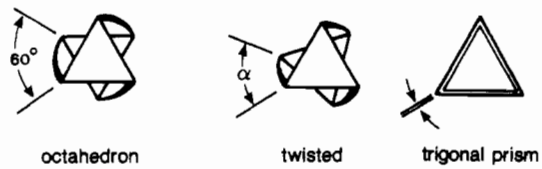

Figure 3. Twist angle α in a tris-bidentate complex $M(LL)_3^{n+}$ and its relation to ideal octahedral and trigonal prismatic geometries.

species, are close to 80° rather than the ideal 90°. There is also generally a small twist away from octahedral to trigonal prismatic geometry. For the tris-gmi cation the bite angle and twist angle are respectively 80.0 and 52.6°, and the corresponding values are 79.5 and 52.9° in the $[Fe(bmi)_3]^{2+}$ species. The twist angle values contrast with 60° for an exact octahedron and 0° for a trigonal prism; see Figure 3 and also ref 28.

Bond lengths, both Fe–N and N⋯C, C⋯C in the chelate rings, for $[Fe(gmi)_3]^{2+}$ and some other iron(II) complexes of symmetrical bidentate diimine ligands are collected together in Table V.[29-32]

Table IV. Solubilities and Transfer Chemical Potentials for $Fe(gmi)_3^{2+}$ in Water and Aqueous Alcohols[a]

	% ROH, v/v				
	20	40	60	80	90
			C_2H_5OH[b]		
$10^3 \times$ solu	45	45	34	9.3	2.2
$\delta_m\mu^\theta$(salt)	0	0	+1.9	+11.7	+23
$2\delta_m\mu^\theta(ClO_4^-)$[c]	+0.4	+1.8	+5.9	+8.6	+12
$\delta_m\mu^\theta$(cation)	−0.4	−1.8	−4.0	+3.1	+11
			i-C_3H_7OH		
$10^3 \times$ solu	45	43	23	3.7	
$\delta_m\mu^\theta$(salt)	0	+0.6	+3.7	+15.3	
$2\delta_m\mu^\theta(ClO_4^-)$[c]	+2.8	+6.4	+10.8	(+18)[d]	
$\delta_m\mu^\theta$(cation)	−2.8	−5.8	−7.1	(−3)	
			t-C_4H_9OH		
$10^3 \times$ solu	45	43	23	3.7	
$\delta_m\mu^\theta$(salt)	0	+0.4	+4.8	+18.6	
$2\delta_m\mu^\theta(ClO_4^-)$[c]	+1.4	+6.0	+7.2	+10.8	
$\delta_m\mu^\theta$(cation)	−1.4	−5.6	−2.4	+7.8	

[a] For $[Fe(gmi)_3^{2+}]$, ϵ = 8600 $cm^{-1}\ mol^{-1}\ dm^3$ at 554 nm; solubilities are given in mol dm^{-3} and transfer chemical potentials, in kJ mol^{-1} on the molar scale; all quantities at 298.2 K. [b] Solubilities in water and in aqueous methanol are given in ref 22. [c] On the TATB assumption.[1,2] [d] Estimated (extrapolated).

The Fe–N bonds in the gmi and bmi complexes are intermediate between the very short bonds in the benzoquinone diimine, bqdi

(28) Blandamer, M. J.; Burgess, J.; Fawcett, J.; Radulovic, S.; Russell, D. R. *Transition Met. Chem. (Weinheim)* **1988**, *13*, 120.
(29) Peng, S.-M.; Chen, C.-T.; Liaw, D.-S.; Chen, C.-I.; Wang, Y. *Inorg. Chim. Acta* **1985**, *101*, L31.
(30) Johansson, L.; Molund, M.; Oskarsson, Å. *Inorg. Chim. Acta* **1978**, *31*, 117.
(31) Garcia Posse, M. E.; Juri, M. A.; Aymonino, P. J.; Piro, O. E.; Negri, H. A.; Castellano, E. E. *Inorg. Chem.* **1984**, *23*, 948.
(32) Baker, A. T.; Goodwin, H. A. *Aust. J. Chem.* **1985**, *38*, 851.

Table V. Bond Distances (Å) in Iron(II)–Diimine Complexes[a]

	in chelate ring			
	Fe–N	N–C	C–C	ref
$Fe(bqdi)_3^{2+}$	1.91_6	1.30	1.46	29
$Fe(gmi)_3^{2+}$	1.95_2	1.27_2	1.42_3	*b*
$Fe(bmi)_3^{2+}$	1.95_6	1.29_2	1.47_7	*b*
$Fe(phen)_3^{2+}$	1.96	1.38	1.38	30
$Fe(bpy)_3^{2+}$	1.97	1.35	1.48	31
$Fe(btz)_3^{2+}$	1.97	1.38_4	1.45_9	32
$Fe(pica)_3^{2+}$ (low spin)	2.01_3[c]	1.42[d]	1.49	33
$Fe(pica)_3^{2+}$ (high spin)	2.19_5			33

[a] Ligands: bqdi = **6**; btz = **7**; pica = **8**. [b] This work. [c] Fe–N(pyridine) = 2.00_2; Fe–N(amine) = 2.02_4. [d] C–N(pyridine) = 1.36_3; C–N(amine) = 1.48_3.

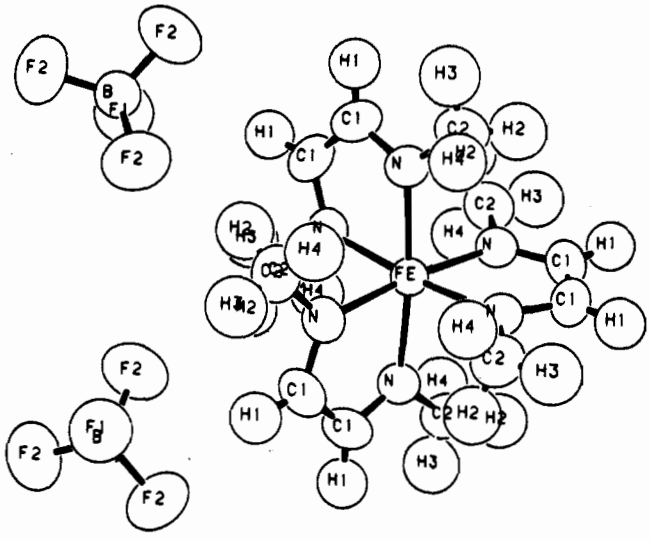

Figure 4. View of $Fe(gmi)_3^{2+}$ down a 3-fold axis.

= **6**, complex and the rather longer bonds in the 4,4′-bithiazole, btz = **7**, complex; further reduction in metal–ligand bond strength results in spin change. Fe–N bonds in high-spin iron(II) complexes are markedly longer, as shown by the tris(2-picolylamine)iron(II) cation[33] (pica = **8**) included for comparison in Table V. Data for both high-spin and low-spin forms of the pica complex are shown in the table. In view of the general correlation between bond length, bond strength, and reactivity with respect to aquation or hydroxide or cyanide attack for these iron(II) complexes, it is surprising that the Fe–N bond lengths are identical within uncertainty limits in the gmi and bmi complexes. This may obscure differences in the σ/π bonding balance, since the other bonds in the chelate rings (Table V) are significantly longer in the bmi complex. Indeed the C–C bond in the Fe–bmi chelate ring, at 1.48 Å, is much nearer the single-bond length in ethane (1.54 Å) than to the double bond of ethene (1.34 Å). The C–C bond in the Fe–gmi chelate ring (1.42 Å) is nearer in length to that in Fe–phen (1.38 Å), itself close to C–C in benzene (1.39 Å). It may well be that there is least π-delocalization in the Fe–bmi ring, so its Fe–N bond is closest to σ-character.

There is no reason to believe that there is any significant change in the geometry of the $Fe(gmi)_3^{2+}$ cation on dissolution of its salts. In particular, proton NMR spectra indicate the presence of six identical C–H protons and six identical methyl groups. The latter signal is at 3.05 ppm in CD_3CN (cf. 2.85, 2.76 ppm for the *N*-methyl ligands of the bmi (**4**, R = R′ = CH_3) and cmi (**4**, R plus R = $-(CH_2)_4-$, R′ = CH_3) analogues.[34] One feature of the structure of $Fe(gmi)_3^{2+}$ that may be significant in relation to its solvation is the clustering of the methyls into groups (Figure 4), leaving voids which may accommodate solvent molecules, particularly small molecules such as water, rather close to the iron at the center of the complex.

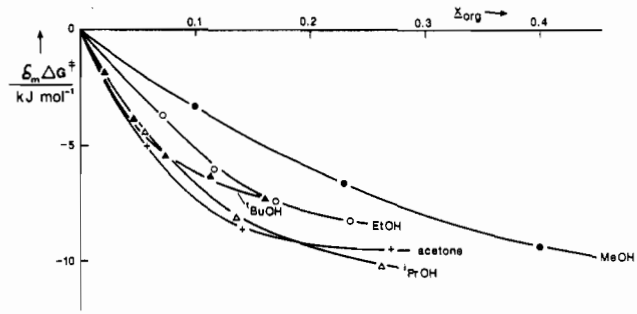

Figure 5. Solvent effects on activation barrier for dissociation by hydroxide of $Fe(gmi)_3^{2+}$ in binary aqueous solvent mixtures. Lines here and in Figures 6–8 are drawn through experimental points for illustrative purposes.

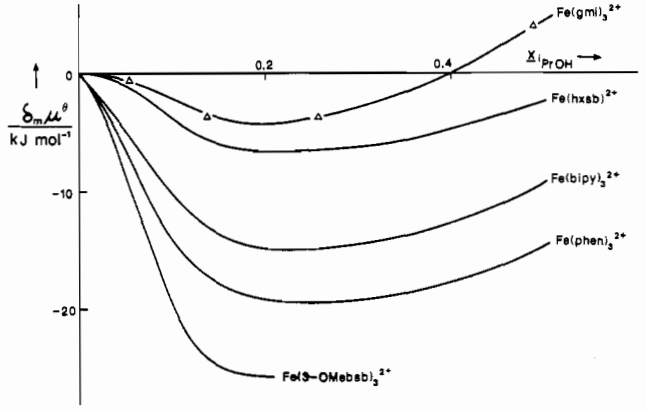

Figure 6. Transfer chemical potentials for transfer of $Fe(gmi)_3^{2+}$ and other iron(II) diimine complexes to aqueous 2-propanol mixtures.

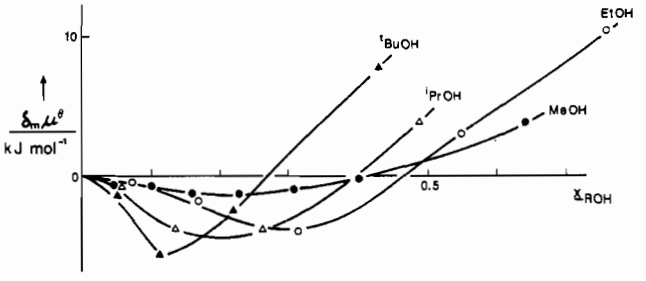

Figure 7. Transfer chemical potentials for transfer of $Fe(gmi)_3^{2+}$ to binary aqueous solvent mixtures.

Kinetics: Atmospheric Pressure. For each individual cosolvent, there is a clear pattern of k_2 increasing with the amount of organic cosolvent, the increase becoming steeper as the proportion of organic cosolvent increases. Plots of k_2 versus volume, weight, or mole percent do not yield a particularly clean-cut pattern of trends for the four alcohols considered and acetone (Figure 5). We therefore need to consider solvent effects on the individual reactants and on the transition state in order to understand the factors contributing.

Transfer chemical potentials for $[Fe(gmi)_3]^{2+}$ from water into aqueous 2-propanol mixtures are shown in Figure 6. In contrast to some other iron(II)–diimine complexes the tris-gmi cation shows rather small solvation changes with change in solvent composition. The trends for $Fe(gmi)_3^{2+}$ resemble those obtained for the moderately hydrophilic $Fe(hxsb)^{2+}$ species. It appears that this uniquely small complex[35] exhibits little preference for water versus alcohols in its solvation shell, in sharp contrast to large hydrophobic

(33) Mikami, M.; Konno, M.; Saito, Y. *Acta Crystallogr.* **1980**, *B36*, 275.
(34) Bayer, E.; Breitmaier, E.; Schwig, V. *Chem. Ber.* **1968**, *101*, 1594. Ito, T.; Tanaka, N. *J. Inorg. Nucl. Chem.* **1970**, *32*, 155. Goedken, V. *Inorg. Synth.* **1980**, *20*, 87.
(35) $Fe(HN{=}CHCH{=}NH)_3^{2+}$ is not available. For a discussion of the status of complexes containing this smallest diimine ligand, see the following: Ali, R. B.; Burgess, J.; Kotowski, M.; van Eldik, R. *Transition Met. Chem. (Weinheim)* **1987**, *12*, 230–235.

Table VI. Activation Volumes ($\Delta V^{\ddagger}$) for Dissociation by Hydroxide of Iron(II)–Diimine Complexes in Aqueous Solution at 298.2 K

complex	$\Delta V^{\ddagger}$, cm^3 mol^{-1}	ref
$Fe(gmi)_3^{2+}$	+16.7	this work
$Fe(phen)_3^{2+}$	+14.2	41
$Fe(3\text{-}CH_3bsb)_3^{2+}$	+13.6	41
$Fe(hxsb)^{2+}$	+13.4	6
$Fe(bpy)_3^{2+}$	+12.8	41
$Fe(4\text{-}CH_3Obsb)_3^{2+}$	+12.0	41
$Fe(3,4\text{-}(CH_3)_2bsb)_3^{2+}$	+11.1	6

cations such as $Fe(3\text{-}OCH_3bsb)_3^{2+}$, bsb = **9**,[36] and, indeed, in less extreme contrast with $Fe(phen)_3^{2+}$ and $Fe(bpy)_3^{2+}$.[22] Figure 7 suggests that the apparent small preference of $Fe(gmi)_3^{2+}$ for a mixed-solvent environment is closely tied to the structures of these binary aqueous media. The shallow minima in the plots of $\delta_m\mu^{\theta}$ ($Fe(gmi)_3^{2+}$) against the mole fraction of alcohol correspond to solvent compositions where the structure of the respective mixtures is generally believed to be maximal.[37]

Transfer chemical potentials for the hydroxide ion have been reported earlier.[38] They show an increase as the amount of organic cosolvent increases, with the effects of organic cosolvent, expressed in mole fractions, increasing in the order CH_3OH < C_2H_5OH < $i\text{-}C_3H_7OH$ < $t\text{-}C_4H_9OH$ < acetone. In subsequent work we expect to address these trends in the overall context of base hydrolysis of organic and inorganic compounds.

Differences between the general trends for the reactant species mean that the transfer chemical potential trends for the initial state for the $[Fe(gmi)_3^{2+}] + OH^-$ reaction are unlikely to give a clear pattern (cf. vide supra). Nonetheless the $\delta_m\mu^{\theta}(OH^-)$ values are generally larger and may be expected to make a major contribution to determining reactivities by increasing the initial-state potential and thereby tending to decrease the activation barrier in higher alcohol content media.

Combining the thermodynamic data for the reactants with the kinetic data for the reaction permits us to separate the solvent effects into initial- and transition-state contributions. This is done for ethanol, 2-propanol, and *tert*-butyl alcohol and water mixtures, in Table IV. A parallel analysis for methanol–water mixtures has been published.[23] For each cosolvent the transfer chemical potential for the initial state in most cases represents a balance between hydroxide destabilization and rather smaller stabilization of the complex cation. In all cases the transition state is stabilized on transfer from water to aqueous alcohol, by an amount not dissimilar from the transfer chemical potential of $Fe(gmi)_3^{2+}$. The incorporation of the very small OH^- into the transition state produces an entity with only 1+ net charge but which otherwise bears a marked resemblance to the iron complex. Indeed one can think of the transition state as $[Fe(OH)(gmi)_3^{+}]^*$. This similarity of the transition state to the starting iron(II) complex is more dramatic for the $Fe(phen)_3^{2+} + OH^-$ reaction. Both $Fe(phen)_3^{2+}$ and $[Fe(OH)(phen)_3^{+}]^*$ are markedly stabilized by the methanol component of the mixed solvents. Both are much more affected than their gmi analogues, since solvation is determined by the strongly hydrophobic nature of the phen ligands, in both initial and transition states.

Activation Volumes

Aqueous Solution. Activation volumes for hydroxide attack at iron(II)–diimine complexes in aqueous solution are listed in Table VI.[23,39-41] The value for the gmi complex, +16.7 cm^3 mol^{-1}, is slightly higher than those we have measured for the other complexes, but since our range is quite small, +16.7 to +11.7 cm^3 mol^{-1}, and the error associated with these particular measurements is typically 10%, an attempt to explain these differences quantitatively would not be realistic. The most important feature of these values is that they are all very different from an "ideal" value of about −10 cm^3 mol^{-1} for the intrinsic activation volume for a bimolecular process; it is generally accepted that the reaction is of associative character whereby a hydroxide ion attacks at the central iron. Therefore, the component of $\Delta V^{\ddagger}$ relating to solvation changes is of the order of +20 to +30 cm^3 mol^{-1}. As has been discussed before, desolvation of the hydroxide ion on entering the transition state appears to be the major factor. If this contribution is independent of the complex, then the range indicated above reflects differences in desolvation of the particular iron complex; by this argument the small gmi complex loses more water to the bulk solvent as the charge changes from plus two to an incipient plus one than does the bulky hydrophobic $Fe(3,4\text{-}(CH_3)_2bsb)_3^{2+}$ species for a comparable charge change. The other complexes having intermediate character in terms of size and hydrophobic/hydrophilic exterior yield $\Delta V^{\ddagger}$ values in the middle of the range. While remaining associative in character, it is conceivable that hydroxide attack and desolvation could occur at different points along the reaction coordinate for each of the iron complexes. The approach of the hydroxide to the probable point of reaction is through different environments; this is clear from the structural information (vide supra) and a model of the iron(II) tris complex of $3,4\text{-}(CH_3)_2bsb$. So while the $\Delta V^{\ddagger}$ values are primarily due to hydroxide desolvation, the differences could be a consequence of minor contributions from varying desolvation components.

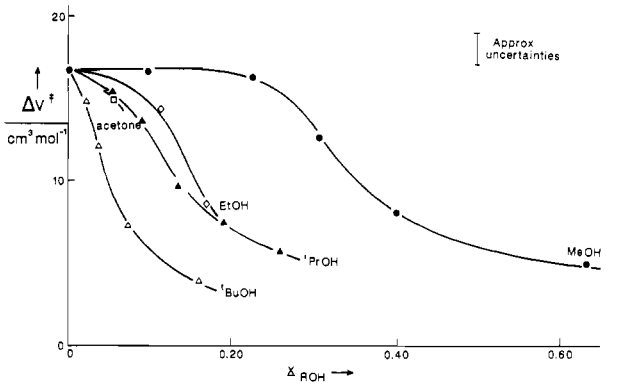

Figure 8. Dependence of activation volume on medium for dissociation by hydroxide of $Fe(gmi)_3^{2+}$ in binary aqueous solvent mixtures.

Aqueous Alcohols. Activation volumes for the $Fe(gmi)_3^{2+} + OH^-$ reaction in aqueous alcohol mixtures (from data in Table III) are plotted against solvent composition (Figure 8). The overall pattern is similar to that established[37] earlier for the hexadentate Schiff base (**10**) complex $Fe(hxsb)^{2+}$, with a decrease in $\Delta V^{\ddagger}$ occurring as water content decreases. The reduction in $\Delta V^{\ddagger}$ is more pronounced at smaller mole fractions of cosolvent for alcohols having a larger organic moiety. The decreases toward, but never approaching (unlike the case for $Fe(hxsb)^{2+}$) the intrinsic value may arise through the hydroxide ion having less water of hydration to lose. The difference for each alcohol is a manifestation of this effect occurring at earlier x_{ROH} for overall less hydrophilic alcohols. This variation in desolvation of the hydroxide ion, contributing to the $\Delta V^{\ddagger}$ changes, is consistent with the kinetic consequence of varying destabilization of hydroxide ion by alcohol cosolvent. The variation of effect with alcohol mole fraction may be related to the mole fraction points of water structure change, caused by alcohol, varying with alcohol.[37]

The effect of cosolvent upon hydroxide cannot wholly explain the variations in $\Delta V^{\ddagger}$; otherwise the trends for $Fe(gmi)_3^{2+}$ would be repeated for other complexes except for cases where transition states are earlier or later than one another. The interpretation of $\Delta V^{\ddagger}$ trends should be compatible with the description of solvation emerging from the values for $\delta_m\mu^{\theta}$ and the initial-state–transition-state analysis. Table IV and other data[22] illustrated in Figure 7 show that $Fe(gmi)_3^{2+}$ is not strongly solvated by water

(36) Blandamer, M. J.; Burgess, J.; Guardado, P.; Hubbard, C. D. *J. Chem. Soc., Faraday Trans. 1* **1989**, *85*, 735.
(37) Franks, F.; Ives, D. J. G. *Q. Rev. Chem. Soc.* **1966**, 1.
(38) Blandamer, M. B.; Briggs, B.; Burgess, J.; Elvidge, D.; Guardado, P.; Hakin, A. W.; Radulović, S.; Hubbard, C. D. *J. Chem. Soc., Faraday Trans. 1* **1988**, *84*, 2703.
(39) Lawrence, G. A.; Stranks, D. R.; Suvachittanont, S. *Inorg. Chem.* **1979**, *18*, 82.
(40) Burgess, J.; Hubbard, C. D. *Inorg. Chem.* **1988**, *27*, 2548.
(41) Burgess, J.; Galema, S. A.; Hubbard, C. D. *Polyhedron* **1991**, *10*, 703.

or alcohols and is weakly solvated (~−2 to −5 kJ mol^{-1}), compared with its state in water, in the region x_{ROH} from 0.1 to 0.4. At higher mole fractions the cation is destabilized; however, high-pressure kinetics measurements are not practicable in these mixtures. The results of Table IV show that the transition states in each aqueous alcohol mixture are slightly stabilized compared with those in water. Therefore, ΔV^* should reflect a decrease in desolvation relative to reaction in water for the $Fe^{II}(gmi)_3$ cation in aqueous alcohols. The results in Table III are qualitatively in agreement with this comparison of solvation probes. It is doubtful whether the partial contribution of each to ΔV^*_{solv} can be assessed quantitatively without detailed models and theoretical description.

The ΔV^* trends for the two small iron(II) cations, $Fe(gmi)_3^{2+}$ and $Fe(hxsb)^{2+}$ (for example, in 60% *i*-C_3H_7OH and 50% *t*-C_4H_9OH, ΔV^* is 4 and 8 cm^3 mol^{-1} less for $Fe(hxsb)^{2+}$), are different. The exterior of $Fe(hxsb)^{2+}$ is not particularly hydrophobic except for the quadrant containing two pyridine rings. By contrast a model of the structure of $Fe(gmi)_3^{2+}$ reveals two close groupings of each of three methyl moieties; thus, the fraction of total surface area that is hydrophobic, while still small, is higher in $Fe(gmi)_3^{2+}$ than in $Fe(hxsb)^{2+}$. This difference, and cation size difference, and the fact that $Fe(hxsb)^{2+}$ has potential hydrogen-bonding sites, could well be the sources of variation in ΔV^*. It could also be speculated that the decline of ΔV^* to a fairly similar value in each alcohol mixture is a reflection of an earlier transition state in which less desolvation occurs and is consistent with the increase in rate constant.

In contrast, the very large and hydrophobic $Fe((CH_3)_2bsb)_3^{2+}$ cation is progressively strongly solvated by methanol with increase in x_{CH_3OH}, as reported earlier.[20] For reaction with hydroxide ΔV^* increases to ~+25 cm^3 mol^{-1} (0–80% CH_3OH), implying a big contribution from methanol desolvation in the transition state; it is not clear why this occurs, unless the solvation of the complex is perturbed in the region of penetration by the charged hydroxide ion, since an overall charge reduction would not favor such desolvation. Size of the alcohol, as well as its intrinsic character may be a factor, since when the higher alcohols are used, while ΔV^* is increased over that for reaction of hydroxide with $Fe((CH_3)_2bsb)_3^{2+}$, the increase is much less pronounced, typically half as much as the same parameter in aqueous methanol. Results from other complexes being studied may lead to development of a clearer interpretation of results.

Acknowledgment. We thank the Royal Society and the SERC for grants toward the purchase and the construction of the Unicam SP 8-100 instrument and the high-pressure apparatus, respectively. The National Science Foundation grant (CHE-7908399) used for purchase of the Cary 219 spectrophotometer is gratefully acknowledged. C.D.H. thanks the Faculty Development Committee of the University of New Hampshire for a travel grant, and support from the British Council (P.G.) is greatly appreciated.

Supplementary Material Available: Listings of bond angles, bond lengths, fractional atomic coordinates, atomic thermal parameters, and nonbonded contacts (5 pages); tables of structure factors (7 pages). Ordering information is given on any current masthead page.

Contribution from the Departments of Chemistry, Iowa State University, Ames, Iowa 50011, and Texas A&M University, College Station, Texas 77843

Chains of Centered Metal Clusters with a Novel Range of Distortions: Pr_3I_3Ru, Y_3I_3Ru, and Y_3I_3Ir

Martin W. Payne, Peter K. Dorhout, Sung-Jin Kim, Timothy R. Hughbanks,* and John D. Corbett*

Received August 26, 1991

The phases R_3I_3Ru (R = La, Pr, Gd, Y, Er) and R_3I_3Ir (R = Gd, Y) are obtained from the reactions of R, RI_3, and Ru or Ir for 3–4 weeks in sealed Ta tubing at 850–975 °C, depending on the system. The title phases have been characterized by single-crystal X-ray means at room temperature, with space group $P2_1/m$ and $Z = 2$ (Pr_3I_3Ru, Y_3I_3Ru, Y_3I_3Ir, respectively: a = 9.194 (1), 8.7001 (4), 8.6929 (7) Å; b = 4.2814 (5), 4.1845 (2), 4.2388 (4) Å; c = 12.282 (2), 12.1326 (6), 12.092 (2) Å; β = 93.46 (1), 94.769 (5), 94.73 (1)°; R/R_w = 3.7/3.4, 3.2/5.5, 4.4/4.0%). The first phase contains quasi-infinite double chains of edge-sharing $Pr_6(Ru)$ octahedra that are sheathed and interbridged by iodine. An evidently continuous distortion of these chains parallels the a/b axial ratio (in the order listed in the first sentence) such that metal octahedra are no longer obvious in Y_3I_3Ir; rather chains of trans-edge-sharing square pyramidal Y_4Ir units bonded base-to-base are more apt. Increased R–R, R–interstitial, and interstitial–interstitial bonding appears to parallel the degree of distortion. Magnetic data for La_3I_3Ru and Pr_3I_3Ru and the results of extended Hückel band calculations on Pr_3I_3Ru are reported. Polar covalent Pr–Ru interactions and at least a quasi-closed shell configuration are emphasized by the latter.

Introduction

A most unusual and prolific chemistry is obtained when rare-earth-metal (R) halides—iodides especially—are reduced in the presence of many of the later transition metals. The dominant structural elements in the products are R_6I_{12}-type octahedral clusters that are either interconnected by iodide in $R(R_6I_{12})$[1] or R_6I_{10}[2,3] stoichiometries or condensed through shared trans metal edges into quasi-infinite chains of clusters. A most remarkable feature is that each cluster is centered by a transition-metal atom. The condensed structures are typified by the La_4I_5Ru and Pr_4I_5Z (Z = Co, Ru, Os) groups recently reported. These are predicted to be metallic according to band calculations.[4] Phases in which such chains are further condensed side-by-side to yield double chains have been long known in other systems, such as Sc_7Cl_{10}[5] and $Sc_7Cl_{10}C_2$[6] (=$Sc_6Cl_7C_2{\cdot}ScCl_3$) and, more recently, $Y_6I_7C_2$,[7] $Gd_6I_7C_2$,[8] etc. The present article reports the first details regarding a different variety of double-chain phases that are now centered by 4d or 5d transition metals. The La_3I_3Ru and Pr_3I_3Ru examples are most analogous to the earlier structures just noted, while, in the distorted relatives Y_3I_3Ru, Y_3I_3Ir, and others, metal octahedra sharing trans and side edges can no longer be easily recognized.

Experimental Section

The purities of the starting metals, the sources of high-quality RI_3 reactants, the synthetic techniques utilizing sealed niobium containers, and the Guinier powder pattern methodology were as described earlier.[1-4]

Syntheses. The specific conditions leading to the black R_3I_3Z phases reported herein in high yield in 3–4 weeks are as follows. La, Ru:

(1) Hughbanks, T.; Corbett, J. D. *Inorg. Chem.* **1988**, *27*, 2022.
(2) Hughbanks, T.; Corbett, J. D. *Inorg. Chem.* **1989**, *28*, 631.
(3) Payne, M. W.; Corbett, J. D. *Inorg. Chem.* **1990**, *29*, 2246.
(4) Payne, M. W.; Dorhout, P. K.; Corbett, J. D. *Inorg. Chem.* **1991**, *30*, 1467, 3112.
(5) Poeppelmeier, K. R.; Corbett, J. D. *Inorg. Chem.* **1977**, *16*, 1107.
(6) Hwu, S.-J.; Corbett, J. D.; Poeppelmeier, K.R. *J. Solid State Chem.* **1985**, *57*, 43.
(7) Kauzlarich, S. M.; Hughbanks, T.; Corbett, J. D.; Klavins, P.; Shelton, R. N. *Inorg. Chem.* **1988**, *27*, 1791.
(8) Simon, A. *J. Solid State Chem.* **1985**, *57*, 2.

0020-1669/92/1331-1389$03.00/0